THREE DIMENSIONAL GLOBAL NONLINEAR TIME HISTORY ANALYSES OF INSTRUMENTED BRIDGES TO VALIDATE CURRENT BRIDGE SEISMIC DESIGN PROCEDURES

Anoosh Shamsabadi[1,*] Tom Ostrom[1] and Ertugrul Taciroglu[2]

[1]Office of Earthquake Engineering,
California Department of Transportation, Sacramento, CA

[2]Civil & Environmental Engineering Department
University of California, Los Angeles, CA

Abstract

California Department of Transportation (Caltrans) and California Geological Survey (CGS) have instrumented a number of bridges, and have been collecting their strong motion response measurements for more than two decades (Hipley and Huang, 1997). The deployed instrument sets usually include down-hole sensor arrays, and accelerometers installed on piles, pile-caps, and decks. These bridges are located relatively close to faults identified on the Caltrans Seismic Hazard Map (Mualchin, 1996). The intent has been to select different bridge types, ranging from standard ordinary bridges to those such as toll bridges with unique features.

This paper presents three-dimensional *global* high-fidelity numerical (finite element) models for three representative bridges—namely, a standard ordinary non-skewed bridge, a skewed bridge, and a non-standard long-span bridge. There are multiple sets of acceleration records due to nearby earthquakes for each of the selected bridges. We carefully, albeit heuristically, calibrate the parameters of these models to improve the agreement between the measured and predicted responses. Upon model calibration, the calculated displacement responses of the simulation models match remarkably well with those obtained from the acceleration records at major locations on the specimen bridges.

Introduction

The main objective this paper is to explore the recorded seismic responses of various types of instrumented bridges, and to improve the current seismic analysis procedures and guidelines through comparisons of recorded responses with predictions from forward simulation models. The primary metrics in these comparisons are the natural frequencies, vibration modes and damping.

Herein, two “standard ordinary” bridges and a “nonstandard bridge” (Caltrans SDC, 2013) are selected for detailed analysis. The *Meloland Road Overcrossing* (MRO)—located near El Centro, California—is the selected non-skewed ordinary standard bridge; the *Painter Street Overcrossing* (PSO)—located in Rio Dell, California—is the selected ordinary standard bridge with a high (39^o) abutment skew angle; and the *Samoa Chanel Bridge* (SCB)—located in

* Presenting Author (Email: anoosh_shamsabadi@dot.ca.gov).

Humboldt County, California—is the selected long-span nonstandard bridge. MRO was constructed in 1971. It is a two-span reinforced concrete box-girder bridge supported on a single-column bent and integral (monolithic) abutments. PSO is a two-span cast-in-place prestressed reinforced concrete box-girder bridge supported by integral abutments and a two-column bent. The SCB consists of 20 spans with four pre-stressed reinforced concrete I-girder supported on single-column bents, and seat-type non-skewed abutments.

Description of Investigated Bridges

MRO is approximately 208 ft long and 34 ft wide with each span measuring 104 ft. The depth of the deck is 5.5 ft. The height of its 5ft-diameter column is approximately 21 ft, which is supported on 25 timber piles with a square concrete cap. The monolithic abutment backwalls have a height of the approximately 13 ft. Each abutment is supported on a single row of 7 timber piles. A photograph of MRO and a schematic showing the locations of its seismic sensors (on deck and abutments) are displayed in Figure 1. Figure 2 displays an idealized soil profiles for MRO along the piles and behind the abutments that were used in our analyses.

Figure 1. Meloland Road Overcrossing (top) and its seismic instrumentation (bottom).

PSO is approximately 265 ft long and 52 ft wide with spans measuring 146 ft and 119 ft with a 39^{o} skew angle. The depth of the deck is 5.67 ft. The average height of the columns is approximately 24 ft, and each is supported on a 4×5 arrangement of concrete piles. The average height of the monolithic abutment backwall is approximately 12 ft. The west abutment wall rests on a neoprene bearing strip lubricated with grease to allow thermal movement between the abutment wall and the backfill. There is a 1 inch gap between the abutment wall and the abutment backfill. The west abutment is supported on a single row of 16 concrete piles. The east abutment backwall is monolithic—i.e., the wall is cast to the deck and the pile-cap, and it is supported on a single row of 14-ton driven concrete piles. The locations of the seismic sensors on the bridge deck and abutments are shown in Figure 3. Figure 4 displays the idealized soil

profile along the piles and behind the abutments. Table 1 summarizes the engineering properties of the existing backfills and natural soils for PSO that were used in the analyses.

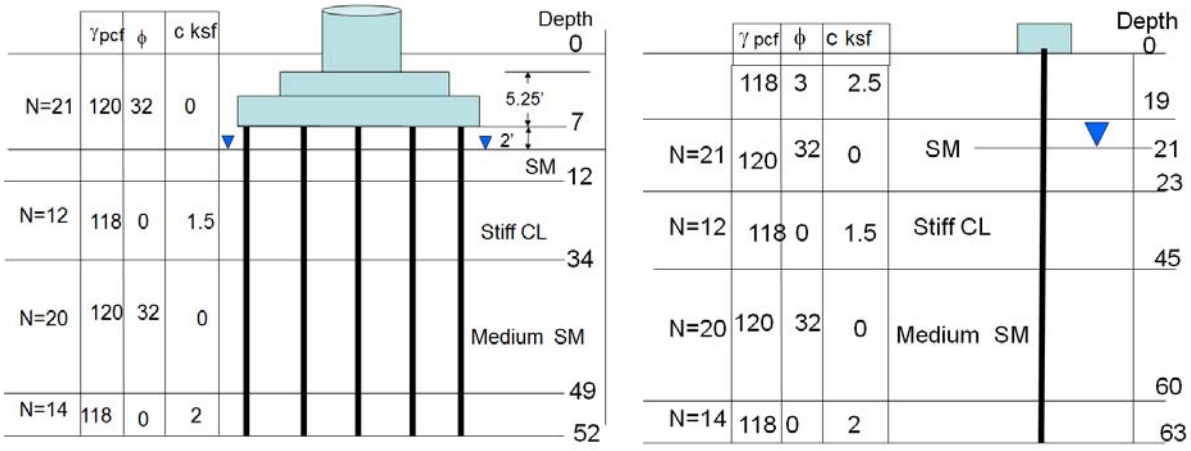

(a) Soil profile along pile group at the bent (b) Soil profile along pile group at abutments

Figure 2. Idealized soil profile for the Meloland Road Overcrossing.

Figure 3. The Painter Street Overpass (top) and its seismic instrumentation (bottom).

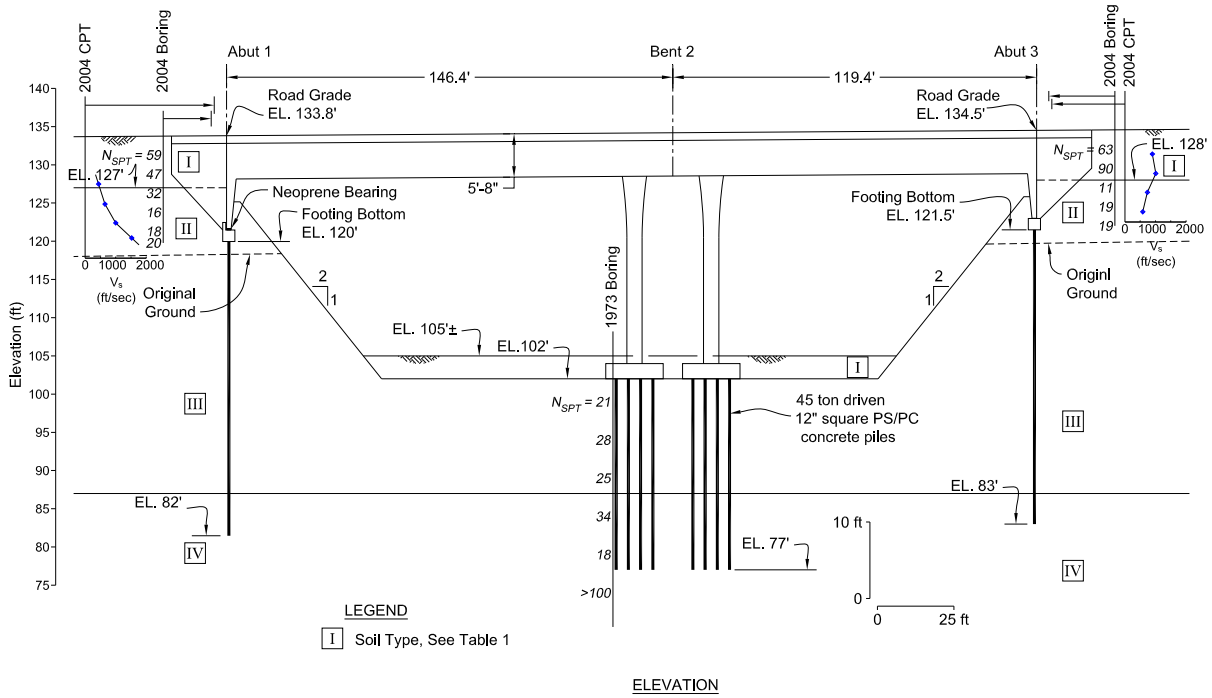

Figure 4. The geometry and idealized soil profile for the Painter Street Overpass.

Table 1. Soil properties for the Painter Street Overpass.

Type	Soil Type (USCS Symbol)	Soil Properties					*p-y* Curve Parameters			Soil Stiffness		
		γ' pcf	ϕ deg	c psf	ν -	v_s fps	k pci	ε_{50} -	J -	E_s ksf	E_{50} ksf	E_r ksf
I	Compacted Sandy Fill (SP, GP)	130	38	50	0.35	670	60	-	-	n/a	n/a	n/a
II	Stiff Silt and Clay (ML/CL)	128	11	3,300	0.40	1,000	-	0.005	0.5	90	110	300
III	Medium dense Sand (SP)	57	34	0	0.35	n/a	60	-	-	n/a	n/a	n/a
IV	Dense Sand with Gravel (SP)	63	36	0	0.35	n/a	80	-	-	n/a	n/a	n/a

Notes: γ' = Effective Unit Weight, ϕ = Friction Angle, c = Cohesion, ν = Poisson ratio, ε_{50} = Strain Parameter for p-y curve, J = Empirical Coefficient for *p-y* curve, v_s = Shear wave velocity, k = Modulus of subgrade reaction, E_{50} = Stiffness at 50% of Ultimate Stress, E_r = Unloading/ Reloading modulus.

The SCB carries Route 225, linking the city of Eureka to Samoa Peninsula (Figure 5). It was constructed in 1971 (construction started in 1968) and underwent a seismic safety retrofit in 2002 (Caltrans, 2002). The bridge is approximately 2506 ft long and 34 ft wide. The locations of the seismic sensors on the bridge deck and the piers, and the basic soil profile at the bridge site are shown on Figure 5. Detailed soil profile data for the SCB are omitted here for brevity, but can be accessed through the California Strong Motion Instrumentation Program's (CSMIP) internet-accessible database (cf. CSMIP Station No. 89734).

The SCB superstructure comprises 6.5in-thick concrete deck slabs resting on four pre-stressed precast concrete I-girders with intermediate diaphragms. The composite deck is supported on concrete bent-cap and hexagonal single-columns and seat-type abutments. The bridge consists of 20 spans. The typical span length is 120 ft except the main channel, which is

225ft-long, and extends from the centerline of pier 8 to the centerline of pier 9. The 150ft-long concrete I-girders of the superstructure begin at pier 7 and pier 10, and are cantilevered 30ft past piers 8 and 9 into the main-channel crossing span. The 165ft-long pre-stressed precast concrete I-girders resting atop the cantilevered portions cross over the main-channel (Figure 5, bottom).

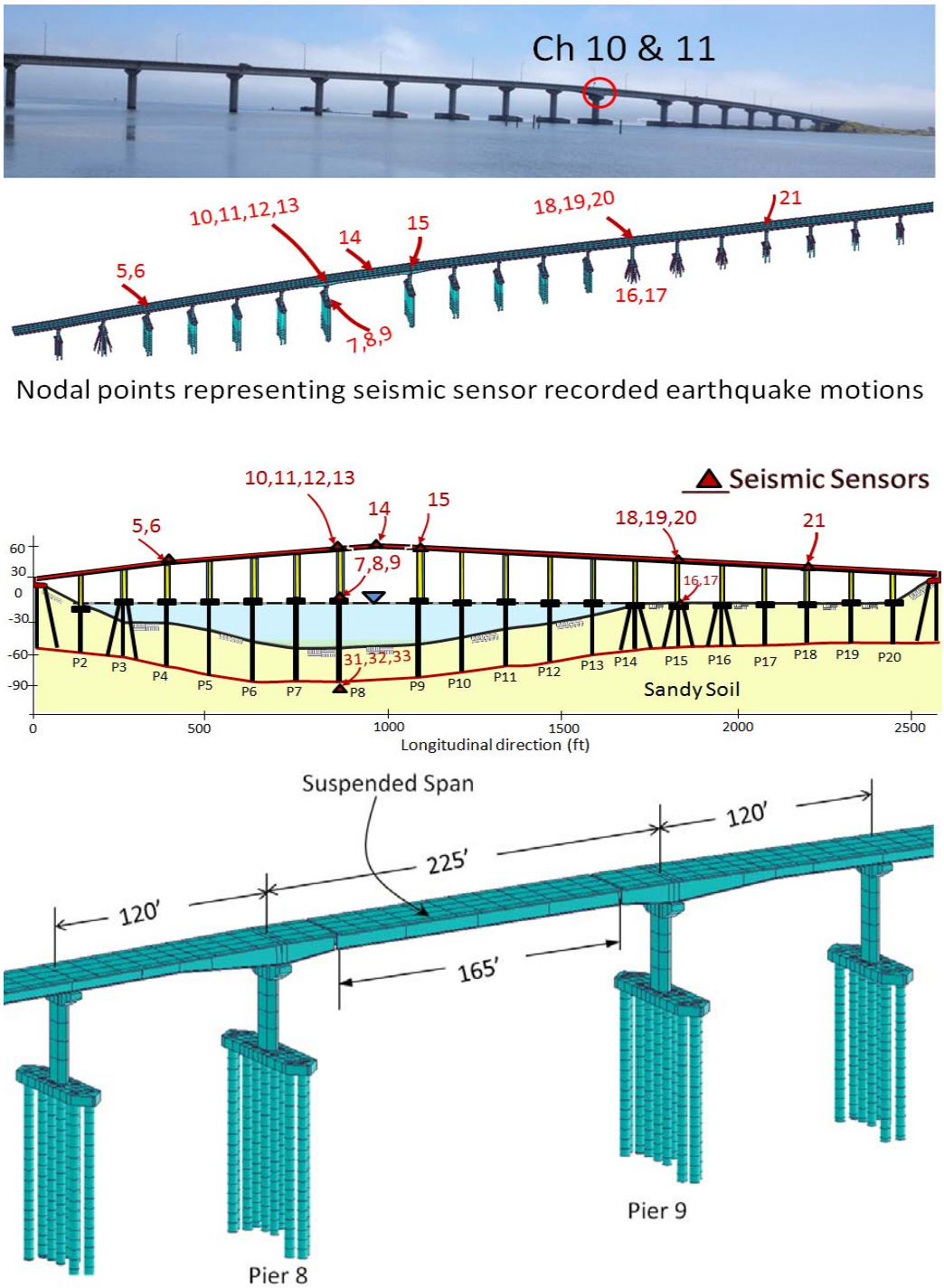

Figure 5. Samoa Channel Bridge (top), its seismic instrumentation (middle), and a close-up view of its finite element model at the main channel crossing.

Bridge Finite Element Models

Detailed global three-dimensional finite-element models of all three bridges were developed (see Figure 6) using the *Midas Civil* (MIDASoft, 2012) computer program. These models featured macroelements to simulate the nonlinear foundation-soil-interaction effects at the abutments and the pile foundations, as well as elements for abutment shear keys. The bridge deck and the abutment walls were modeled as shell elements with appropriately chosen structural properties.

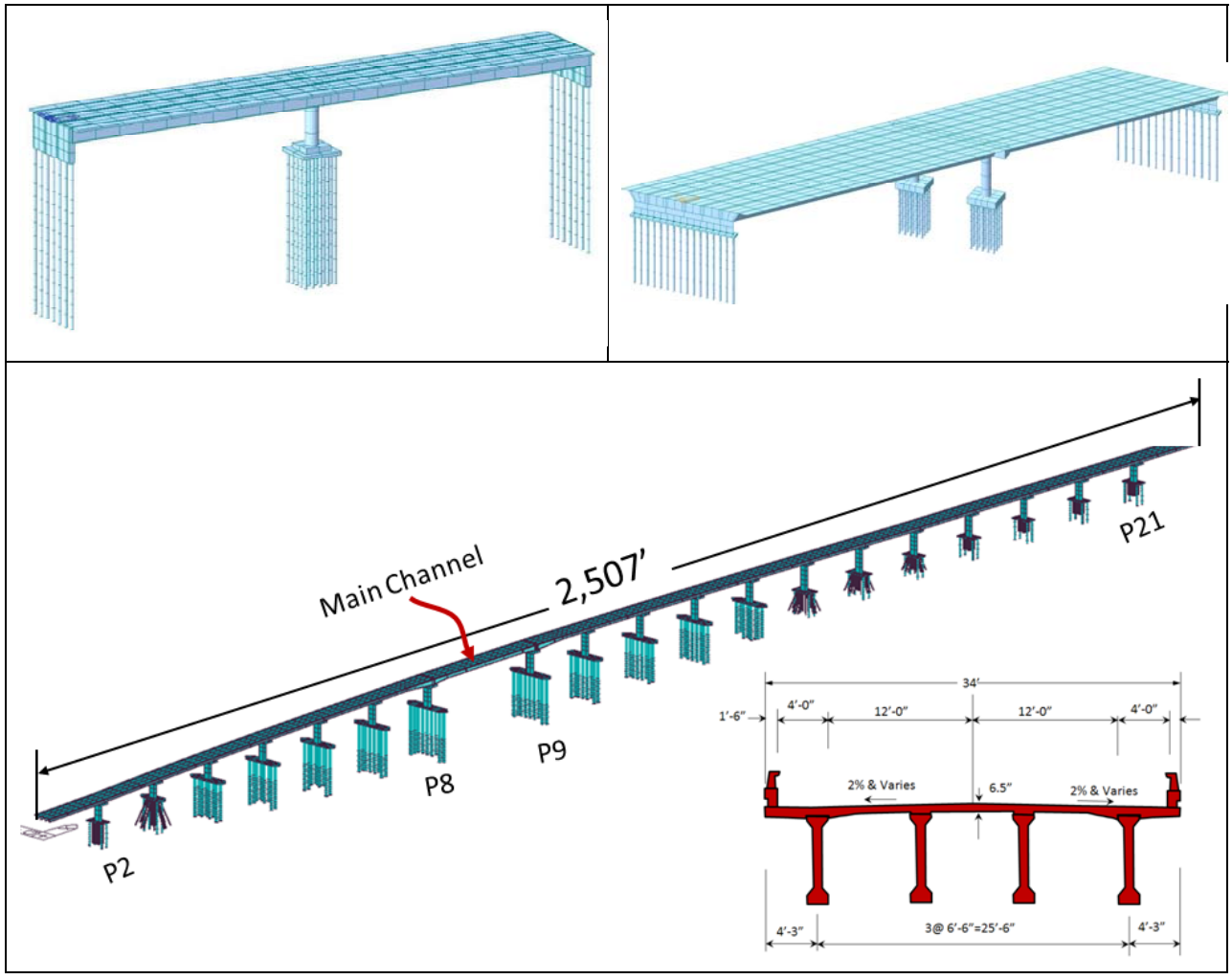

Figure 6. The three-dimensional finite element models of the Meloland Road Overcrossing (top left), Painter Street Overpass (top right), and the Samoa Channel Bridge (bottom).

Abutment and Pile Models

The bridge abutments play a significant role in the global seismic behavior of bridges. This is especially true for ordinary, short-span, bridges like MRO and PSO. For the longitudinal nonlinear spring at the abutment-embankment soil interface, a separate continuum finite-element

model was developed using the computer code PLAXIS with a strain "hardening-soil" model (Vermeer and Brinkgreve, 1998) to develop abutment backbone curves and cyclic unloading-reloading rules (Figure 7a,b) for both the MRO and PSO (a 39^o skew angle was used for PSO).

The behavior of the abutment shear keys in the transverse direction was developed based on a prior Caltrans-UCSD field experiment dataset (Bozorgzadeh et al., 2006, Shamsabadi A, 2007). The nonlinear backbone curve was scaled to produce the structural shear-key capacity of the abutment as a function of displacement between bridge deck and abutment pile-cap (Figure 7b). At the tail-end of the curve, a fourth segment was added to account for the tangential component of the abutment-backfill passive capacity due to deck rotation and the passive capacity contribution of the exterior embankment soil.

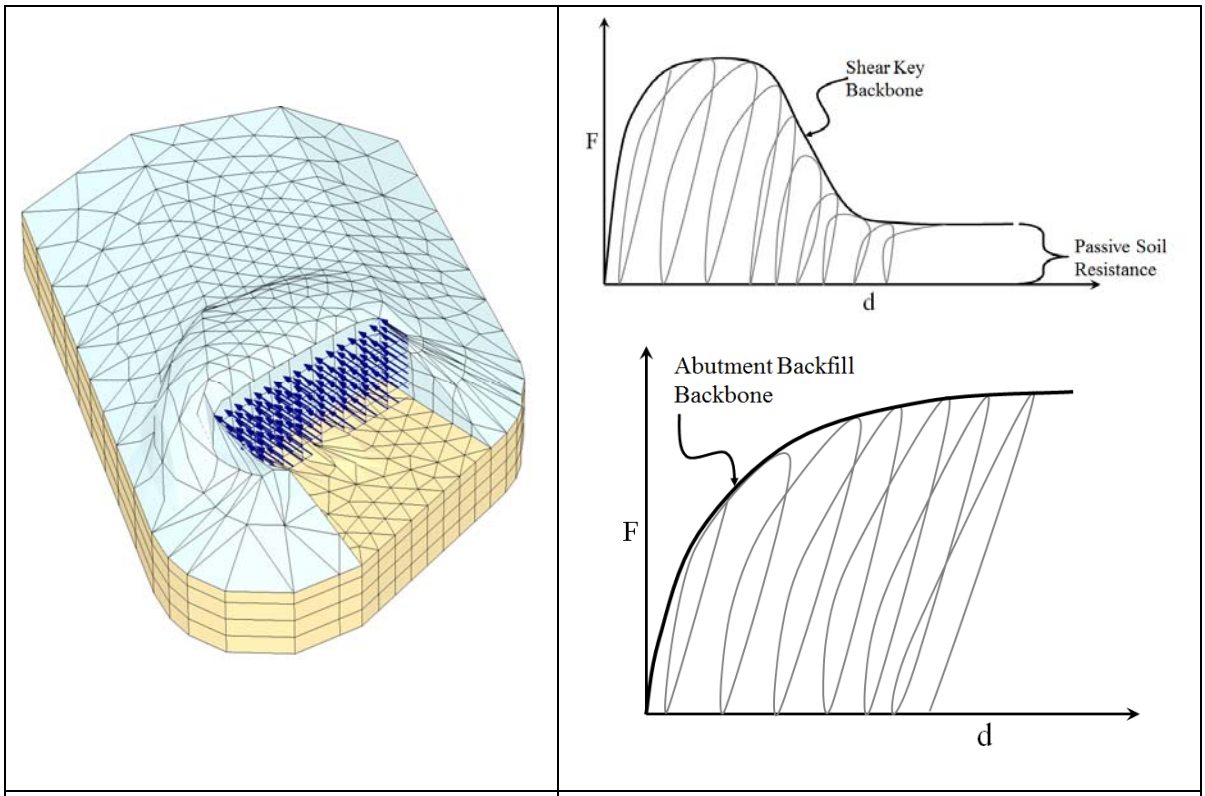

(a) 3D abutment-embankment FEM mesh with the PLAXIS "Hardening-Soil" model.	(b) Transverse and longitudinal backbone and hysteretic cyclic loading-unloading curves.

Figure 7. Ingredients used in modeling the abutment systems.

The hysteretic behavior of the backbone curves both in transverse and longitudinal directions were modeled using a multi-linear plasticity model with the tension side of the curve set to zero. The transverse shears keys were modeled using a single spring attached at each corner of the abutment. The longitudinal abutment-backfill was modeled by a series of nonlinear link elements distributed along each abutment backwall in the bridge global models as shown in Figure 8.

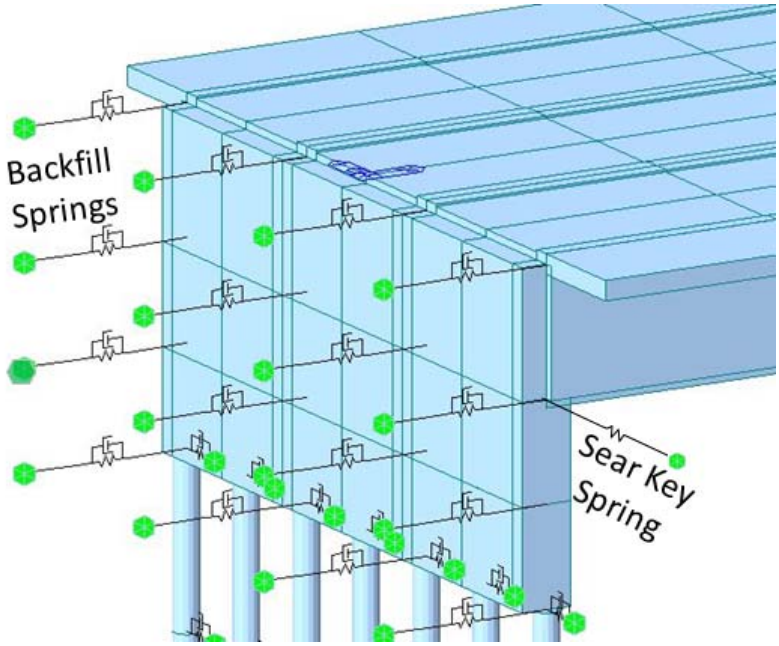

Figure 8. Distributed longitudinal and transverse abutment springs in the bridge models.

The support provided by the west abutment of PSO was modeled using a friction isolator to simulate the neoprene pad, and to decouple the superstructure and abutment backwall from the pile-cap. The isolator is fixed in the vertical direction only. The support provided by the east abutment is fixed to the pile-cap.

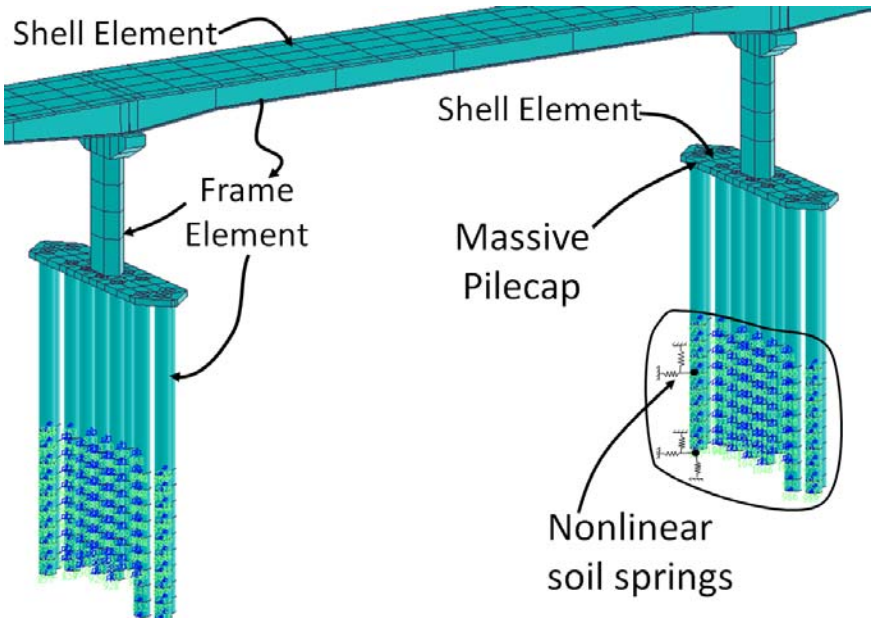

Figure 9. The nonlinear soil springs used in the finite element model of the SCB.

The pile foundations were modeled as beam elements with depth-varying nonlinear springs to represent the interaction between the piles and surrounding soil. Figure 9 displays a close-up view of the global bridge model for of Piers 8 and 9 for the SCB. The fully three-dimensional nonlinear model includes all structural components, foundation components and three-component nonlinear soil support springs. The nonlinear soil springs (Matlock 1970; API 1993) were developed using site-specific geotechnical data (CSMIP, 2012). The soil springs are not only nonlinear but also inelastic upon unloading to allow for hysteretic behavior of the soil. Because the pile caps are massive, the seismic response of the foundations to the earthquake has been found to be an important factor when matching the response of the 3D global model with the recorded seismic response of the bridge.

Input Motions

For dynamic analyses of the MRO, the recorded free-field accelerations from the April 4, 2010 Baja California earthquake were used as the input motions (CGS Station 01336). For PSO, input motions were the free-field records of the 1992 Cape Mendocino/Petrolia earthquake (CGS Station 89324). For the Samoa Channel Bridge, free-field accelerations from the magnitude 6.5 January 2010, Ferndale Area earthquake were used (CGS Station 89686). These acceleration records were obtained from the Center for Engineering Strong Motion Data (CESMD) website, which provides public access to acceleration records from a variety of seismic networks (www.strongmotioncenter.org).

Representative Results

On April 2, 2010, the Caltrans Office of Earthquake Engineering and researchers from University of British Colombia (UBC) collected ambient vibration data from various locations on MRO. Those data were subsequently to for estimated the mode shapes and the natural frequencies for the bridge. The modal data calculated using the finite element model versus those extracted from recorded ambient vibration records are shown in Figure 10.

While the various further refinements can be iteratively made to the model, the agreement between the two sets of modal properties is already observed to be remarkably well. This finite element model was subsequently used to predict the displacement time histories obtained from the earthquake acceleration records to further validate the finite element model. Transverse and longitudinal displacements at a representative location on MRO (Channels 9, and 27) are shown on Figure 11, where, again, the agreement between the actual (recorded) and predicted displacements are observed to be excellent for this two-span ordinary bridge.

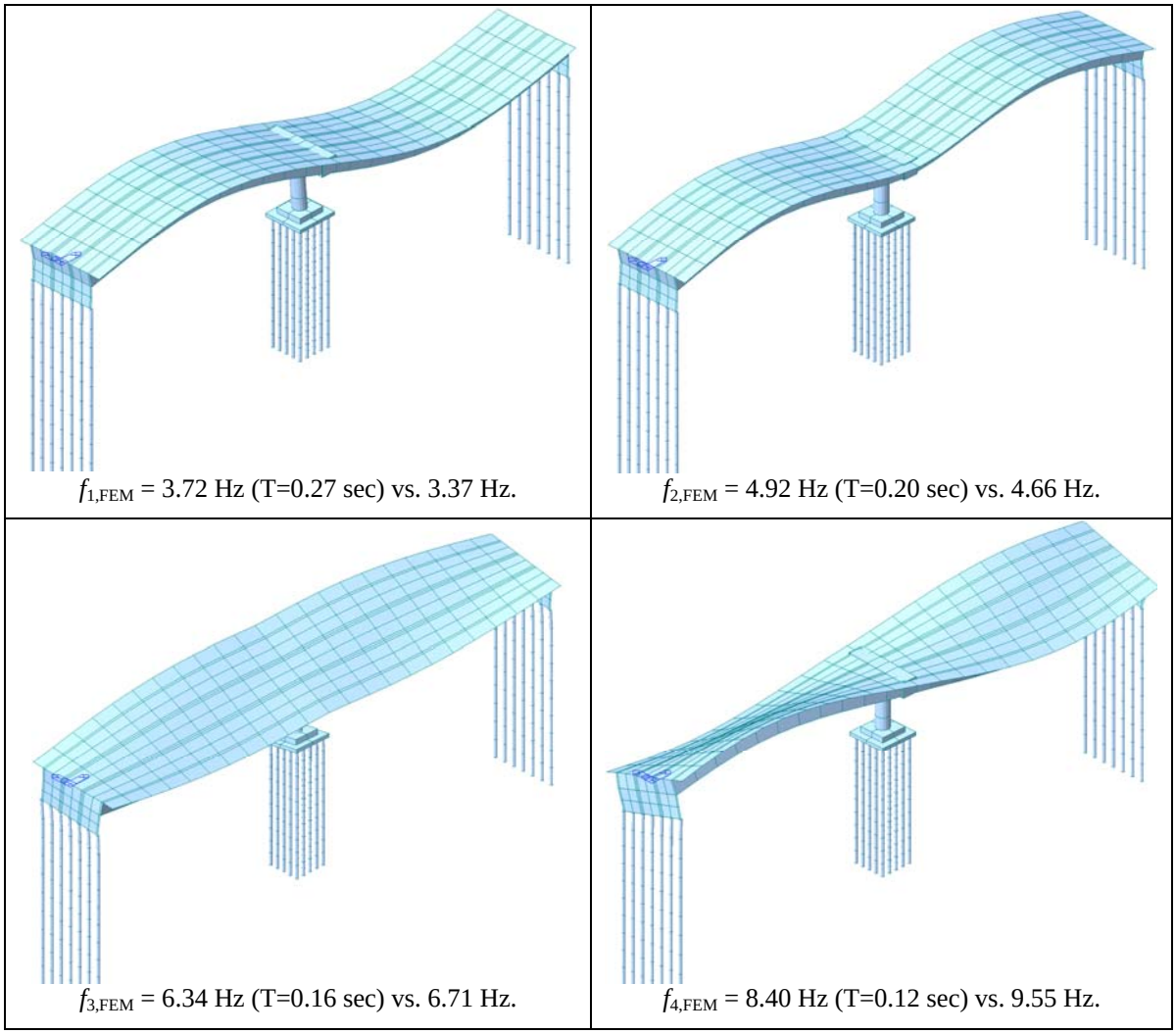

Figure 10. Mode shapes and natural frequencies of the Meloland Road Overcrossing obtained from the initial finite element model versus those extracted from ambient vibration data.

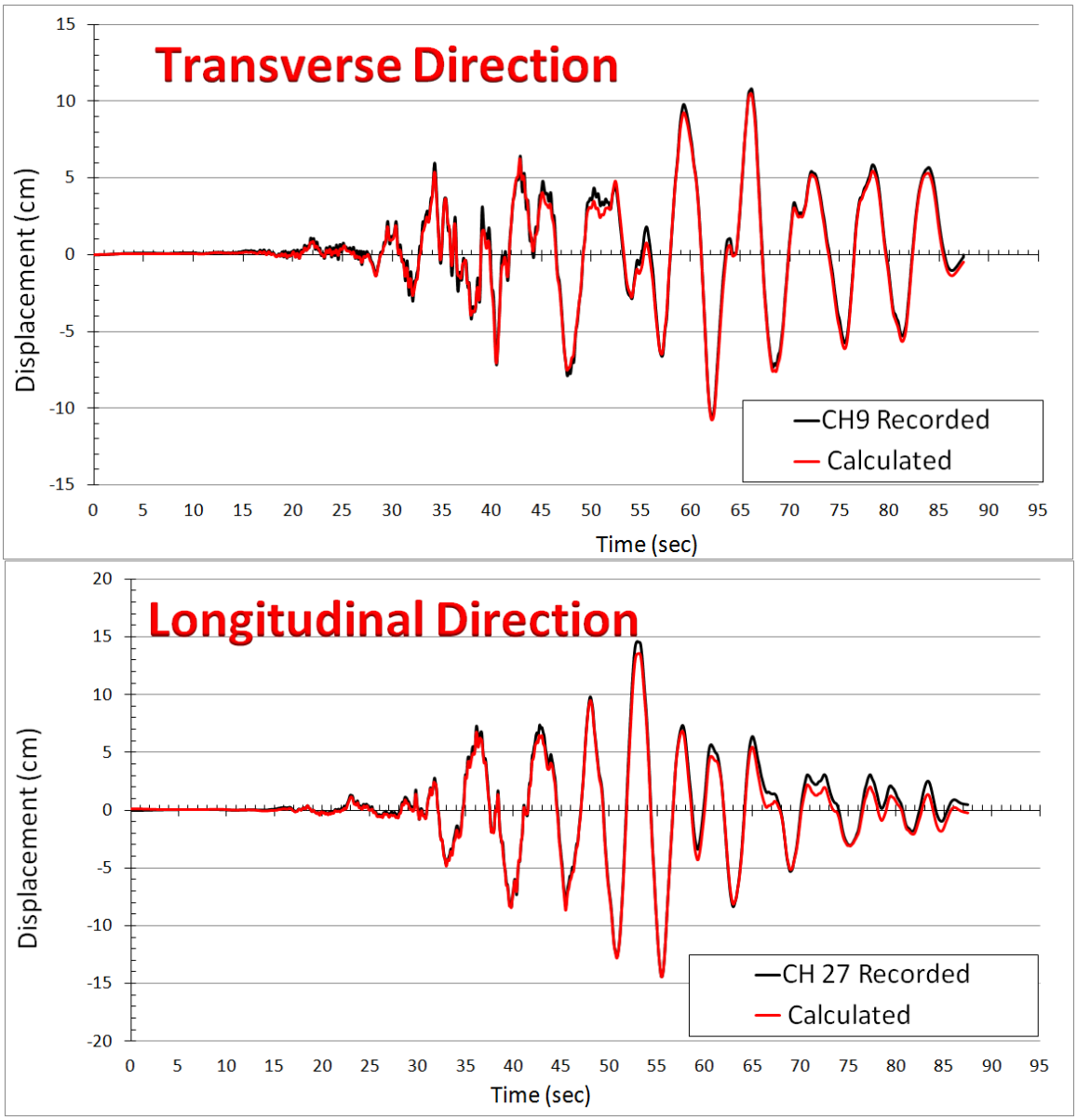

Figure 11. Computed and recorded displacements for the Meloland Road Overcrossing.

The calculated mode shapes and natural frequencies for the Painter Street Overpass are shown in Figure 12. Unlike MRO, we did not have ambient data for the PSO. Therefore, the finite element model was directly used to predict the displacement time histories obtained from earthquake acceleration records for model validation. Transverse and longitudinal displacements at a representative location on PSO (Channels 7, and 11) are shown on Figure 13. Again, the agreement between the actual (recorded) and predicted displacements is observed to be excellent for this two-span ordinary bridge that has a skew abutment. While the considered earthquake motions—*viz.*, recorded motions due to the 1992 Cape Mendocino/Petrolia earthquake—were not severe enough to induce inelastic/permanent deformations, the aforementioned agreement between the predicted and measured responses validate—albeit indirectly—the elastic loading/unloading portions of the abutment-backfill interaction macroelement besides the model of the super-superstructure.

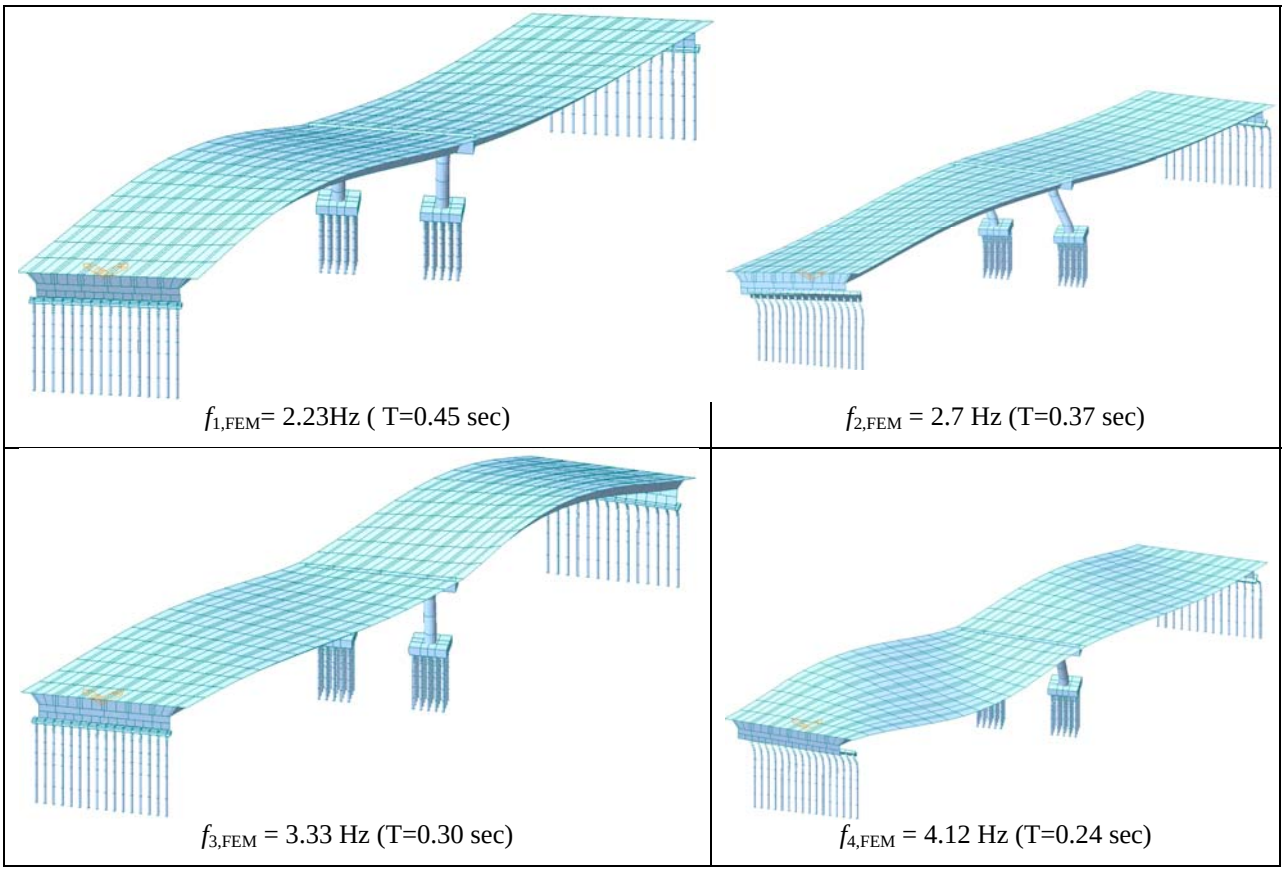

Figure 12. Mode shapes and natural frequencies of the Painter Street Overpass obtained using the initial finite element model.

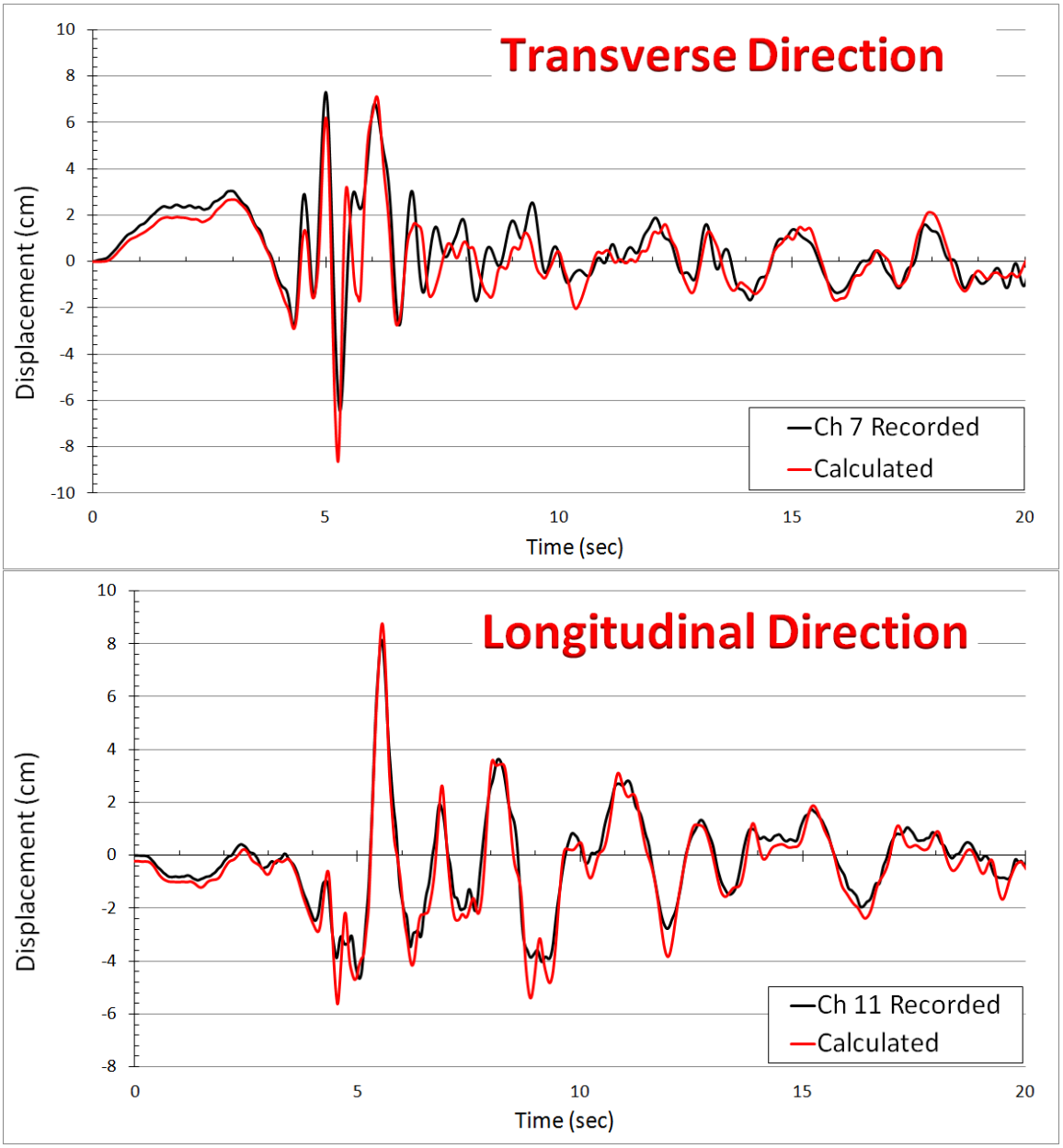

Figure 13. Computed and recorded displacements for the Painter Street Overpass.

The calculated transverse and longitudinal modal data for the Samoa Channel Bridge are shown in Figure 14 (only the first two modes are presented here, for brevity). Unlike the ordinary bridges, the SCB model required multiple iterations from the initial finite element model so that the computed motions matched the recorded motions. The key ingredients in these model-updating studies were the use of cracked section stiffness values for the superstructure elements, the correct values for the mass of the pile caps, and the pile-foundations' lateral stiffnesses. Details of these iterative model-updating studies are omitted for brevity, and may be found in (Shamsabadi et al., 2012). The updated finite element models ultimately displayed very

good agreement with the earthquake-recorded motions. Representative results (Channels 10 and 11) are shown in Figure 15.

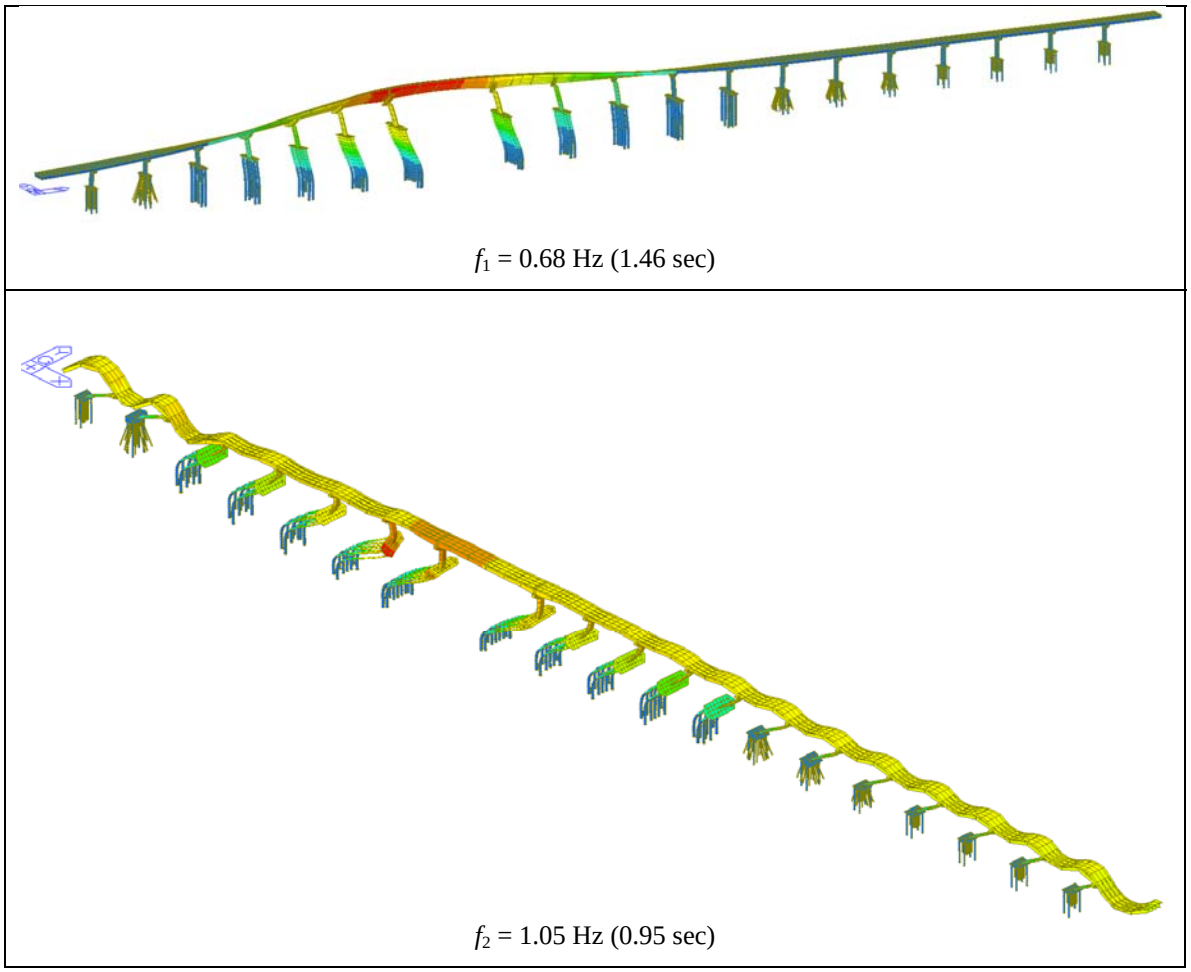

Figure 14. The first two modes of the Samoa Channel Bridge computed using *Midas Civil*.

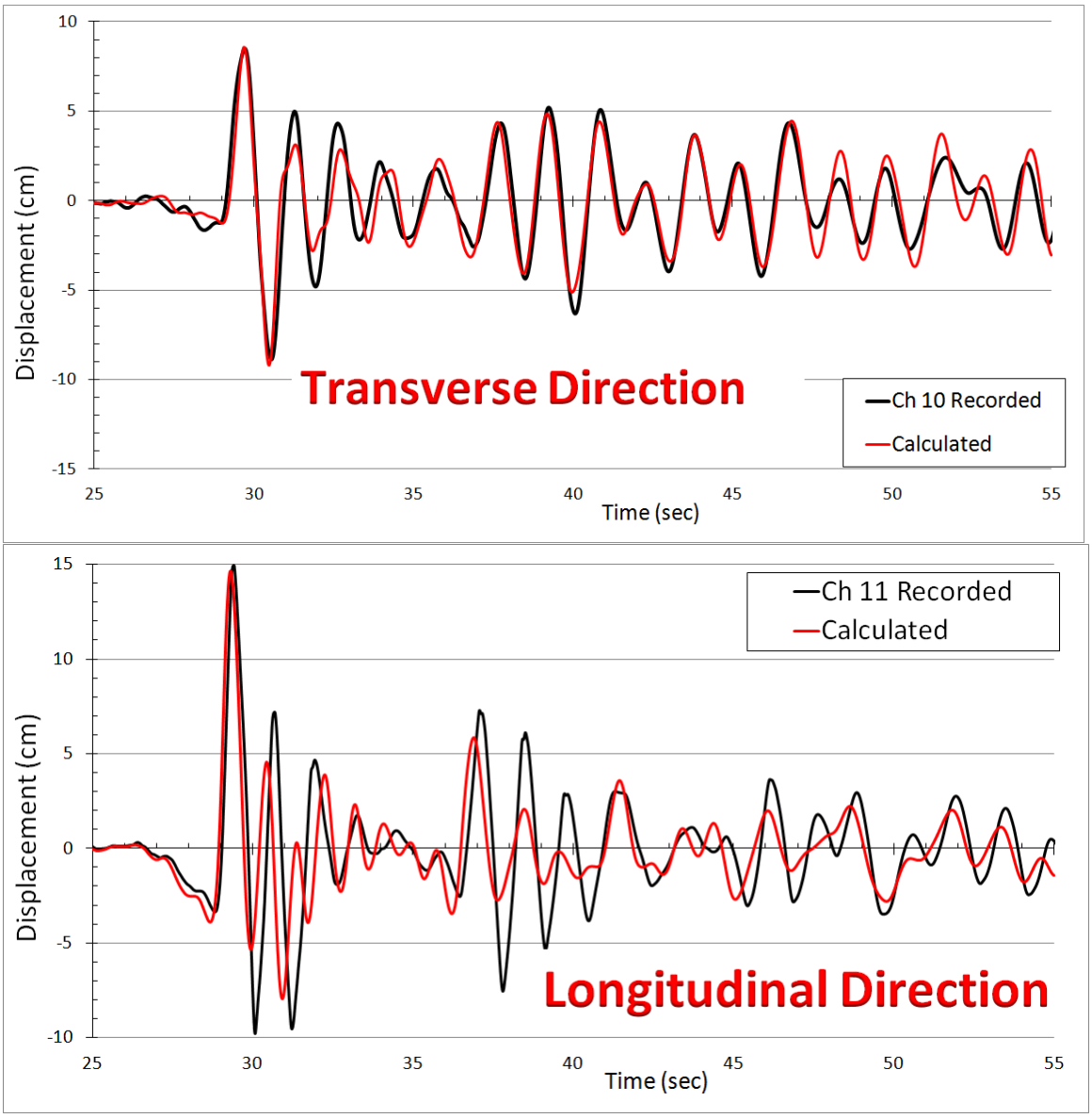

Figure 15. Computed and recorded displacements for the Samoa Channel Bridge.

Conclusions and Recommendation for Future Studies

The ability of finite element models created from structural drawings and geotechnical data in predicting the response of bridges during strong motion events were explored. To this end, three instrumented bridges that are representative of California's bridge inventory were selected. Two of the bridges were ordinary bridges one of which has an abutment with a large (39^{o}) skew angle. The other bridge was a long-span non-ordinary bridge.

Three-dimensional detailed finite element models were developed for the three bridges, which were constructed and analyzed using the *Midas Civil* computer program. These models featured nonlinear/inelastic macroelements that represented the soil-structure interaction at the abutments and pile foundations, as well as the behavior of abutment shear keys. The passive

cyclic response of backfill soils for skew abutments that were used in the macroelements were calibrated using high-fidelity three-dimensional continuum finite element models developed and analyzed using PLAXIS computer program.

The results obtained for the all of the bridges studied suggested that—provided that the abutment and pile foundations are accurately modeled, the finite element models could predict the response observed in strong—albeit non-damaging—earthquakes. The calibration of the finite element model for the long-span bridge was found more challenging, and required more careful consideration of the superstructure properties in comparison to the ordinary bridges. Further studies are needed to clearly delineate the influence of soil-foundation-structure effects in both ordinary and non-ordinary bridges. This can be achieved through parametric studies using validated/calibrated finite element models such as those presented in this study. Moreover, studies are required to investigate the expected behavior of these (and similar) bridges under damaging earthquakes in order to determine the influence of soil-structure effects on the seismic demands that these bridges will be experience.

References

API—American Petroleum Institute (1993), *Recommended Practice and Planning, Designing, and Constructing Fixed Offshore Platforms – Working Stress Design (RP 2A-WSD*), Washington, D.C.

Bozorgzadeh A, Megally S, Restrepo JI, Ashford SA (2006). Capacity evaluation of exterior sacrificial shear keys of bridge abutments, *ASCE Journal of Bridge Engineering*, 11(5): 555-565.

Caltrans SDC (2013). *Caltrans Seismic Design Criteria, v.1.7*, April 2013.

CSMIP (2012). *California Strong Motion Instrumentation Program*, http://www.conservation.ca.gov/cgs/smip.

Hipley P, Huang M (1997). Caltrans/CSMIP bridge strong motion instrumentation. *Second National Seismic Conference on Bridge and Highways*, Sacramento, California.

Matlock, H. (1970), "Correlation for Design of Laterally Loaded Piles in Soft Clay," 2nd Annual Offshore Technology Conference, Paper No. 1204.

Mualchin, L (1996). *A Technical Report to Accompany the Caltrans Seismic Hazard Map 1996 (Based on Maximum Credible Earthquakes)*, California Department of Transportation, Engineering Service Center, Office of Earthquake Engineering, Sacramento, CA 95816.

MIDASoft (2010). *Midas Civil: Integrated Solution System for Bridge and Civil Engineering*, MIDAS Information Technology Co., Ltd. (www.MidasUser.com)

Shamsabadi A. Three–dimensional nonlinear seismic soil–abutment–foundation-structure interaction analysis of skewed bridges, Ph.D. thesis, Department of Civil and Environmental Engineering, University of Southern California (USC), Los Angeles, CA (2007).

Shamsabadi A, Mitchell S, Hipley P, Zha J, Omrani R, Ghahari SF, Abazarsa F, Taciroglu E (2012). Assessment of seismic soil-foundation-structure interaction analysis procedures for

long-span bridges using recorded strong motion data, *Proc. 10th Int. Congress on Advances in Civil Engineering*, Ankara, Turkey, 17-19 October.

Vermeer PA, Brinkgreve RBJ (1998). *PLAXIS: Finite-element code for soil and rock analyses* (version 7.1), Balkema, Rotterdam, The Netherlands.